



Article

Long-Term Change of Coastline Length along Selected Coastal Countries of Eurasia and African Continents

Fan Yang^{1,2,3}, Li Zhang^{1,2}, Bawei Chen^{1,2,*} , Kaixin Li⁴, Jingjuan Liao^{1,2} , Riffat Mahmood⁵,
Mohammad Emran Hasan⁶, M. M. Abdullah Al Mamun^{1,3,7}, Syed Ahmed Raza^{1,3} and Dewayany Sutrisno⁸

¹ Key Laboratory of Digital Earth Science, Aerospace Information Research Institute, Chinese Academy of Sciences, Beijing 100094, China

² International Research Center of Big Data for Sustainable Development Goals, Beijing 100094, China

³ University of Chinese Academy of Sciences, Beijing 100049, China

⁴ School of Marine Technology and Geomatics, Jiangsu Ocean University, Lianyungang 222005, China

⁵ Department of Geography and Environment, Jagannath University, Dhaka 1100, Bangladesh

⁶ Climate Justice and Natural Resource Rights, Oxfam GB in Bangladesh, Mohakhali, Dhaka 1206, Bangladesh

⁷ Institute of Forestry & Environmental Science, University of Chittagong, Chattogram 4331, Bangladesh

⁸ Center for Research, Promotion and Cooperation, Geospatial Information Agency (BIG), Cibinong 16911, Indonesia

* Correspondence: chenbw@aircas.ac.cn; Tel.: +86-010-82178109

Abstract: The acquisition of dynamic coastline change at fine spatial and temporal resolution is essential for enhancing sustainable coastal economic development and coastal environmental conservation. Port construction, land reclamation, urban development, and sediment deposition have resulted in extensive coastline change. In this study, the coastlines along the 56 coastal countries in 1990, 2000, 2010, 2015, and 2020 were delineated and classified into six categories using Landsat time-series images. Five relevant indices, i.e., the length, length ratio, length change rate, index of coastline utilization degree (ICUD), and fractal dimension (FD), were calculated to analyze and explore the spatiotemporal pattern of the coastlines. The results indicate that: (1) The overall length of the coastlines has increased from 3.45×10^5 km to 3.48×10^5 km in the past 30 years, with a net increase of nearly 3904 km. Between 1990 and 2020, the length of the artificial coastline increased by about 13,835 km (4.9~8.8%), while the length of the natural coastline decreased by 9932 km (95.1~91.2%). The increase in artificial coastline is concentrated in Southeast Asia and South Asia. (2) The coastline fractal dimensions (FDs) of countries and continents show that the average FD values of countries in South Asia (1.3~1.4) and Southeast Asia (1.2~1.3) were higher than other countries in the study regions, meaning that the coastlines in South Asia and Southeast Asia are more complex and curved. (3) The value of the ICUD index increased consistently between 1990 and 2015 (177.7~186.6) but decreased sharply between 2015 and 2020 (186.6~162.4), implying that the impact of human activities on the coastline continued to increase until 2015 and began to decrease after 2015. Our study examined the changes in various types of coastlines, which could be significant for sustainable development and environmental protection in coastal areas.

Keywords: coastline change; coastline structure change; fractal dimension; index of coastline utilization degree; land-sea pattern; Landsat imagery



Citation: Yang, F.; Zhang, L.; Chen, B.; Li, K.; Liao, J.; Mahmood, R.; Hasan, M.E.; Mamun, M.M.A.A.; Raza, S.A.; Sutrisno, D. Long-Term Change of Coastline Length along Selected Coastal Countries of Eurasia and African Continents. *Remote Sens.* **2023**, *15*, 2344. <https://doi.org/10.3390/rs15092344>

Academic Editors: Valeria Tomaselli, Maria Adamo and Cristina Tarantino

Received: 2 April 2023

Revised: 19 April 2023

Accepted: 26 April 2023

Published: 28 April 2023



Copyright: © 2023 by the authors. Licensee MDPI, Basel, Switzerland. This article is an open access article distributed under the terms and conditions of the Creative Commons Attribution (CC BY) license (<https://creativecommons.org/licenses/by/4.0/>).

1. Introduction

The coastal zone is the transition zone of land-ocean interactions, which is considered the most complex and dynamic natural surface system. It is heavily influenced by natural and anthropogenic disturbances, and rich in land and marine resources. Thus, the coastal zone is an important and thriving ecosystem that benefits people in many ways, such as fisheries, aquaculture, agriculture, human settlements, harbors, ports, tourism, and industries [1,2]. Global climate change and various natural phenomena, such as erosion,

saltwater intrusion, subsidence, tsunamis and flood, and tropical cyclone [3–5] affect coastal regions. The pressure faced by the coastal zone is not only from natural disasters but also from frequent human activities and rapid social-economic development [6]. Coastal zones have been identified as highly vulnerable in terms of environmental and socioeconomic settings [7]. The majority of the coastal zone is heavily populated due to the spatial clustering of the world's megacities (population > 10 million) [8]. By using the global geospatial grid datasets, researchers have estimated that about 39% of humans all over the world live within 100 km of the coastline [9], and the population density has continually risen in recent decades. Human interaction with infrastructure, city expansion, the development of maritime commerce [10], and other intensive exploitations are often accompanied by maritime disasters and coastline degradation [11,12]. Therefore, the importance of coastline protection and coastal sustainability has been emphasized in recent years [13,14].

Defined as 'the line of the physical interface between land and water body' [15,16], the coastline is an important linear feature for describing the dynamic changes of coasts and coastal degradation due to both natural and artificial factors [17,18]. It is the dividing line between land and sea and is constantly changing due to its unique environmental characteristics. However, the rapid expansion of ports and changes in the population and land use patterns of coastal cities (e.g., fisheries) pose challenges to coastal ecosystems and species diversity, the coastal environment, the socioeconomic activities of local residents, and the tourism industry. Extreme weather and climate-induced changes such as coastal erosion and sea level rise [19,20] are likely to increase the risk of inundation in many parts of the coastal zone, especially over densely populated low-lying areas. Anthropogenic activities (such as marine reclamation, port construction, and tourism development) [21–23], as well as the climate change process and deterioration of the coastal environment in multiple ways (such as mangrove degradation, deforestation, near-shore water pollution, coastal erosion, seawater intrusion, and coral bleaching), tend to destroy coastal resources, alter the coastal environment, reduce the stability of ecosystems, and reshape the coastline [24–27]. At least 70% of the world's beaches show a long-term chronic erosion tendency [28].

The selected areas include more than 50 countries, and most of the countries are located mainly in tropical and subtropical regions. Some of the countries are prone to frequent natural disasters, such as hurricanes and tsunamis, and some have fragile ecosystems [29] that are sensitive and show weak self-recovery [30,31], some are facing severe coastline retreat, and some have ongoing urban development and reclamation activities. In 2015, the United Nations proposed 17 Sustainable Development Goals (SDGs), which provide a shared blueprint for peace and prosperity for people and the planet. Regarding ocean and coastal resources, SDG 14 emphasizes the idea of conserving and sustainably using the oceans, seas, and marine resources. Hence, monitoring coastline changes in coastal countries could provide a better assessment of SDG 14.

This study aimed to assess coastline changes in terms of position and types for 56 coastal countries between 1990 and 2020, using multi-temporal Landsat imagery. With its long history, Landsat imagery has been the most recognized archive for monitoring long-term coastline changes over large areas [32]. However, most of the studies have been focused on delineating the coastline and its temporal change, and few studies have assessed the coastline changes in terms of different types of coastlines. Therefore, this study analyzed and assessed the coastline changes using the metrics of coastline length, length change, coastline change rate, index of coastline utilization degree (ICUD), and fractal dimension (FD) to assess the regional pattern of coastline change and their response to natural and anthropogenic factors. This study provides fundamental information for government officials and coastal managers to construct scientific and rational policies for land use planning and the sustainable development of coastal zones [33,34].

2. Materials

2.1. Study Area

The study area encompasses 3 continents, 13 typical coastal areas, and over 50 countries or regions, with broad spatial scales and significant regional distinction (Figure 1). The countries selected for this study are mainly along the coastal zones of Eurasia and African continents. It was divided into five regions, including Southeast Asia, South Asia, West Asia, the Mediterranean coast, as well as Southeast Africa. Countries with long coastlines, such as Indonesia, the Philippines, Malaysia, and Vietnam, are also included. Most countries and regions are sensitive in the context of climate and geological changes, with very complex natural and fragile ecological environments [35]. Southeast Asia, one of the most biologically diverse and rich regions in the world, is also included, which is affected by typhoons and flooding annually.

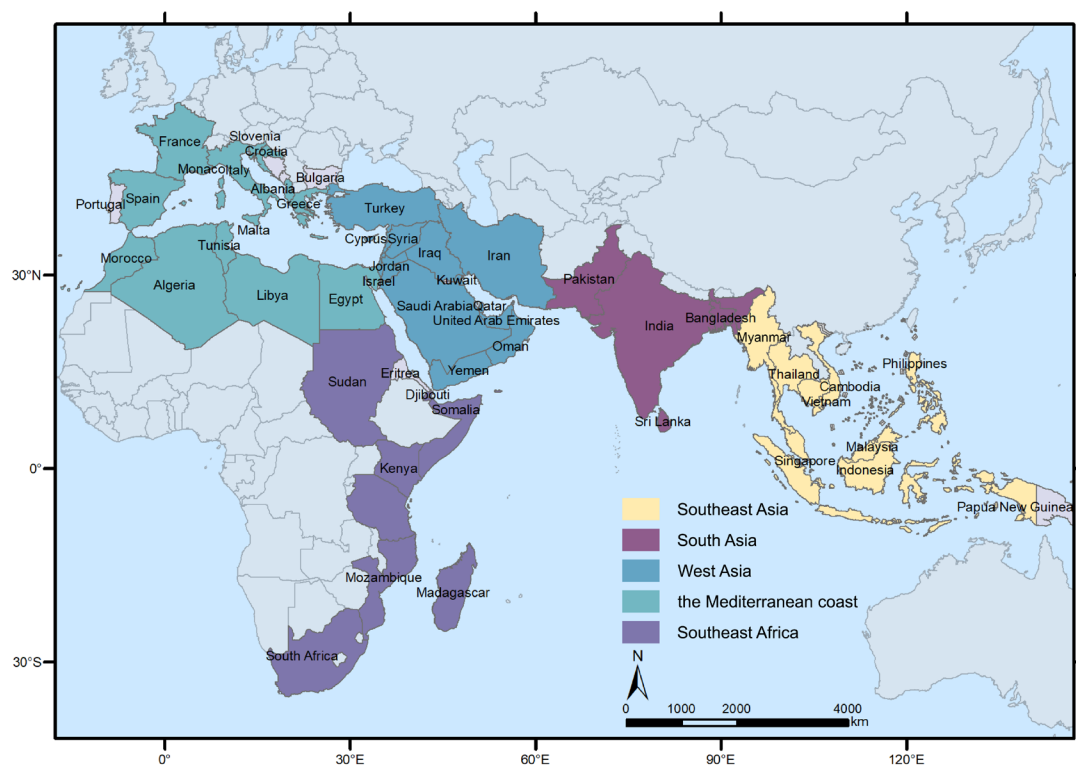


Figure 1. Study area.

2.2. Data Sources

The Landsat series (TM: Thematic Mapper, ETM+: Enhanced Thematic Mapper Plus, and OLI: Operational Land Imager, 30 m) from 1990, 2000, 2010, 2015, and 2020 were used for extracting the coastline datasets. A total of 3872 scenes of Landsat images with good-quality and free of cloud (at least over the coastlines of interest) and sensor defects (striping or banding), covering the entire coast of the study area, were selected for this study via <https://earthexplorer.usgs.gov> (assessed on 15 October 2021). The NIR (near infrared) (0.85–0.88 μm), red (0.64–0.67 μm), green (0.53–0.59 μm) bands were selected to composite false color images, as they provided strong contrast between land and water, so the coastline can be easily identified in remote sensing images.

3. Methods

3.1. Coastline Definition and Classification

Although the definition of coastline is simple and clear, this line is not easily recognized on satellite images. It maintains a dynamic state because of coastal sediment movement, tidal surge, beach erosion, waves, and human activities. Many previous studies have

proposed various practical coastline metrics, such as mean high-water line (MHWL), instantaneous high-water line (HWL), and low-water line (LWL) [36,37]. Among these indicators, the MHWL is the most accepted because of its clear identification and high stability [38]. Thus, these coastline metrics were also used in this paper.

The methods of coastline extraction using remote sensing images can be generally classified into two categories: manual visual interpretation and automatic computer interpretation [39,40]. Although automatic computer interpretation has the advantage of extremely high efficiency and reusability, visual interpretation has the advantages of high interpretation accuracy and continuous extraction of coastlines when distinguishing different categories of coastline and is very resistant to noise when targeting complex areas, which ensures accuracy and precision [41]. This study extracted the coastline data with a manual visual interpretation method, and the banded images were processed in ArcGIS software to outline the coastline with vector data.

At present, there is no definite and acceptable coastline classification system. Based on the literature review, coastlines were classified into five types according to differences in anthropogenic utilization. The broad classification includes artificial coastline and natural coastline. The natural coastlines include biotic coastline, bedrock coastline, estuary coastline, silty coastline, and sandy coastline [42]. Artificial coastlines, such as harbors, reclamation, aquaculture dikes, and beach berms, are usually built at the convergence zone between land and sea for living security and economic development. The coastline classification system and the description of different types of coastlines are presented in Table 1. The specific flowchart for coastline extracting and classification is shown in Figure 2.

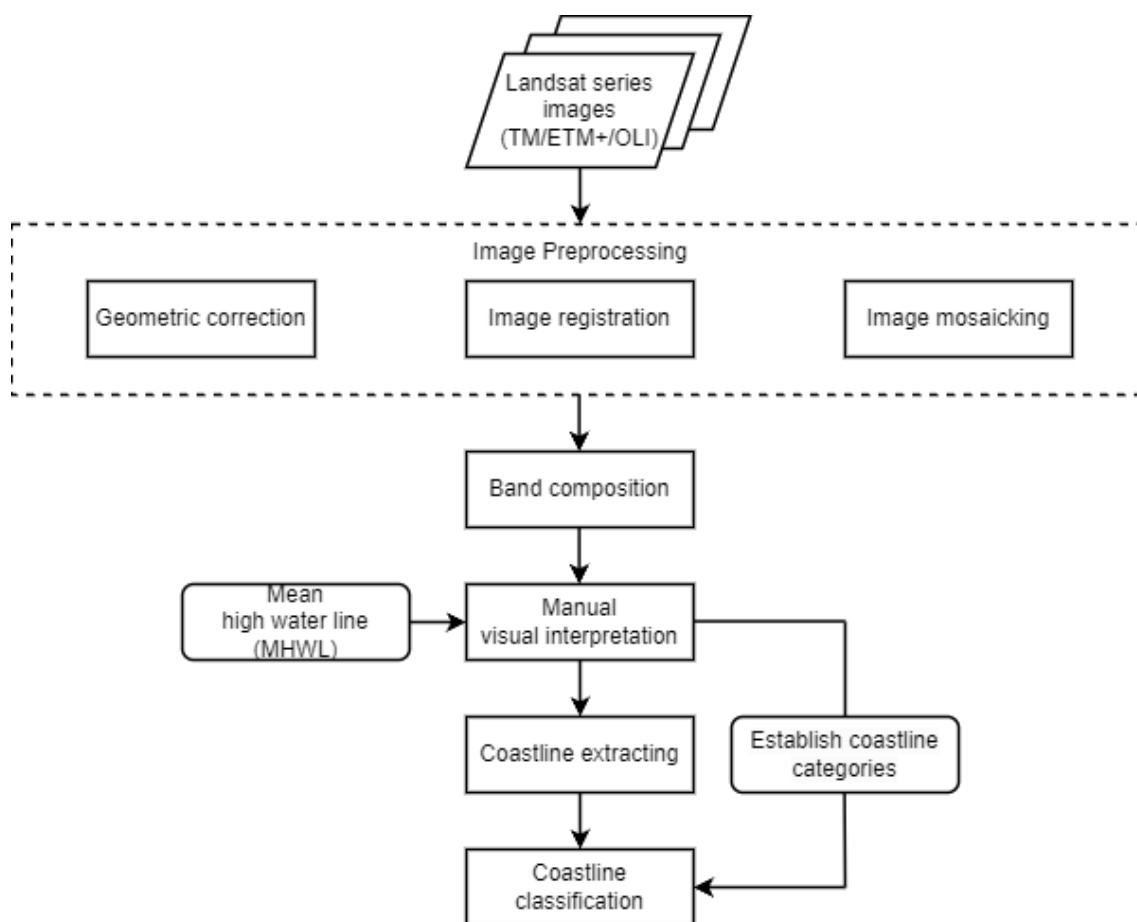


Figure 2. Flowchart of extraction and coastline classification.

Table 1. Coastline categories.

Category		Description	Image Sample
Natural coastline	Bedrock coastline	The coastline distributed on bedrock with a distinct state of undulation, and is relatively tortuous and remains largely unchanged. Bare, steep, and hard rocks cover the surface of this coastline.	
	Biotic coastline	Biotic coastline is usually developed by the role of mangroves and reef-building coral. The seaward side is mostly consisted of mangrove forests, showing some green shore in remote sensing images (no silt, sandy, landward side is not an artificial coastline).	
	Estuary coastline	Estuary coastline is generally located at the entrance of the rivers into the sea. Its boundary is between estuary and ocean, which remains largely unchanged.	
	Sandy coastline	Sandy coastline is mostly located in the open bay. The beach is yellow or off-white, generally smooth and wide. The coastline is long and largely in a state of erosion.	
	Silty coastline	Silty coastline grows in hidden bays, and the shore form is mostly smooth silty beach. The coastline is obviously dark in color, with sediment accumulation and weak hydrodynamic conditions.	
Artificial coastline	Harbors, dikes, jetties, etc.	Artificial coastline is a coastline that has been changed by human action that has altered the original form of its natural state. Obvious artificial coastline includes ports, wharfs, and docks for human activities.	

3.2. Indicators of Coastline Change

3.2.1. Coastline Change Rate (CCR)

The coastline change is widely accepted as a highly reliable and effective indicator to estimate coastline change [43]. We calculated the change in total coastline length over time, the rate of change, and the length ratio and rate of change ratio for each type of coastline. To avoid the effects caused by inconsistent observation intervals and to ensure the consistency of coastline change data, annual average data were used to describe these changes, as shown in this formula:

$$\text{CCR} = \frac{l_2 - l_1}{y_2 - y_1} \quad (1)$$

where l_2 and l_1 represent the length of the coastline for different years, and y_2 and y_1 represent the year they each correspond to.

3.2.2. Index of Coastline Utilization Degree (ICUD)

The ICUD indicates the extent to which the coastline is affected by human actions [44]. According to the impact of human activities on the coastline, different human action intensity indexes are given to different types of coastlines: bedrock coastline = estuarine coastline = 1, sandy coastline = 2, biotic coastline = silty coastline = 3, artificial coastline = 4 [45]. The following formula is used for calculation:

$$\text{ICUD} = \sum_{i=1}^n (A_i \times C_i) \times 100 \quad (2)$$

where n represents the number of types of coastlines; A_i represents the human action intensity index corresponding to the i th type of coastline; and C_i represents the percentage of the length of the coastline of type i . The larger the ICUD, the greater the impact of human actions on the coastline.

3.2.3. Fractal Dimension (FD)

Length is the basic characteristic of the coastline. However, the length of the coastline cannot be used as the indicator of coastline change because there are significant differences in the length of the coastline measured at different scales [46]. The fractal dimension mainly describes the most important parameters of fractal [47]. The higher the fractal dimension is, the higher the curvature and complexity of the coastline are. This study used the grid method [48] to calculate the fractal dimension of the coastline.

Square grids with constant side length r are used to cover the coastlines, and the number of grids ($N(r)$) will inevitably change according to the variable r . In fractal theory, the relationship between the side length of the grid and the number of grids is as follows:

$$N(r) \propto r^{-D} \quad (3)$$

When the length of the grid is set to a series of different values, a series of corresponding grid number sequences are obtained. After taking the logarithms of the two sequences, linear fitting is carried out, and the following formula is obtained:

$$\lg N(r) = -D \lg r + A \quad (4)$$

where A is a constant and D is the fractal dimension of the coastline.

4. Results

4.1. Coastline Length Change

The extracted coastlines derived from the Landsat images between 1990 and 2020 are depicted in Figure 3a. The coastline of the 56 countries showed a general trend of increasing and then decreasing between 1990 and 2020. Figure 3b illustrates the overall coastline

length of 3.45×10^5 km in 1990 to a maximum length of 3.59×10^5 km in 2010 and then decreased to 3.48×10^5 km in 2020. the increase in coastline length over the last 30 years was 3904 km, with an average annual rate of change of 130 km/year.

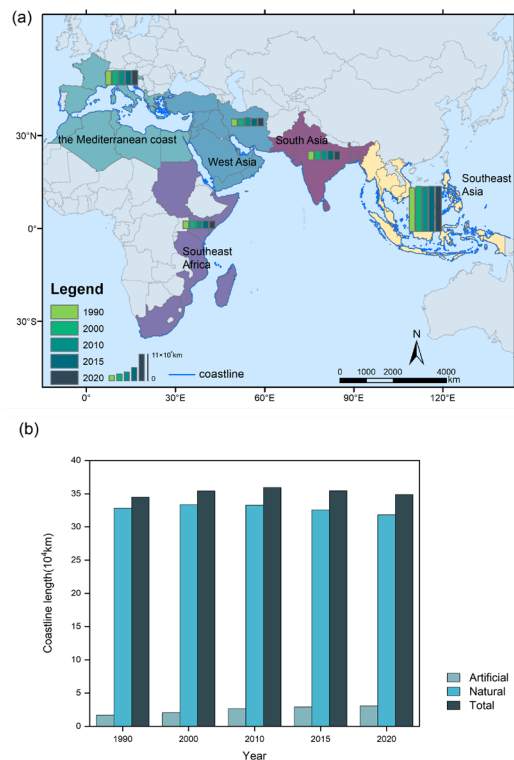


Figure 3. (a) Coastline length changes in five regions (colored as Figure 1) from 1990 to 2020; (b) The length change of artificial and natural coastlines for the 56 coastal countries.

The natural coastline shows a trend of slight increase and then decrease, from 3.28×10^5 km in 1990 to 3.34×10^5 km in 2000, and then decrease to 3.18×10^5 km in 2020. The artificial coastline shows a continuous growth trend, increasing from 1.69×10^4 km in 1990 to 3.07×10^4 km in 2020, an overall increase of 1.38×10^4 km, with an annual rate of change of 461 km/year. Although a rapid increase was revealed in the artificial coastline, the overall length of the coastline of the 56 coastal countries began to decrease slowly after reaching a maximum in 2010. Over the past 30 years, continued development in the dynamic coastal zones induced more natural coastlines to be destroyed, and more artificial coastlines were constructed during that period.

Figure 4 shows the average annual rate of coastline change for each country from 1990–2020. In Southeast Asia, the coastlines of Indonesia and Myanmar are growing rapidly, with an average annual growth rate of 31.8 km/year and 47.2 km/year, respectively, while the coastlines of Malaysia and the Philippines are decreasing with an average annual rate of change of -33.1 km/year and -26.2 km/year. The coastline of countries in Southeast Asia is more variable, with an average annual rate of change of -23.8 km/year for the coastline of Bangladesh and -23.8 km/year for the coastlines of India. Most countries in the West Asia region have positive average annual rates of coastline change, with Saudi Arabia and the United Arab Emirates at 27.7 km/year and 33.8 km/year, respectively. In the Mediterranean region, Greece and Italy have higher average annual coastline growth rates of 28.1 km/year and 36.3 km/year, respectively, while the coastline of Spain shows a greater decrease with an average annual rate of change of -37.9 km/year. Most of the countries in Southeast Africa show a decrease in the coastline, with Eritrea, Mozambique, and South Africa showing average annual rates of change of -22.6 km/year, -16.2 km/year, and -16.4 km/year.

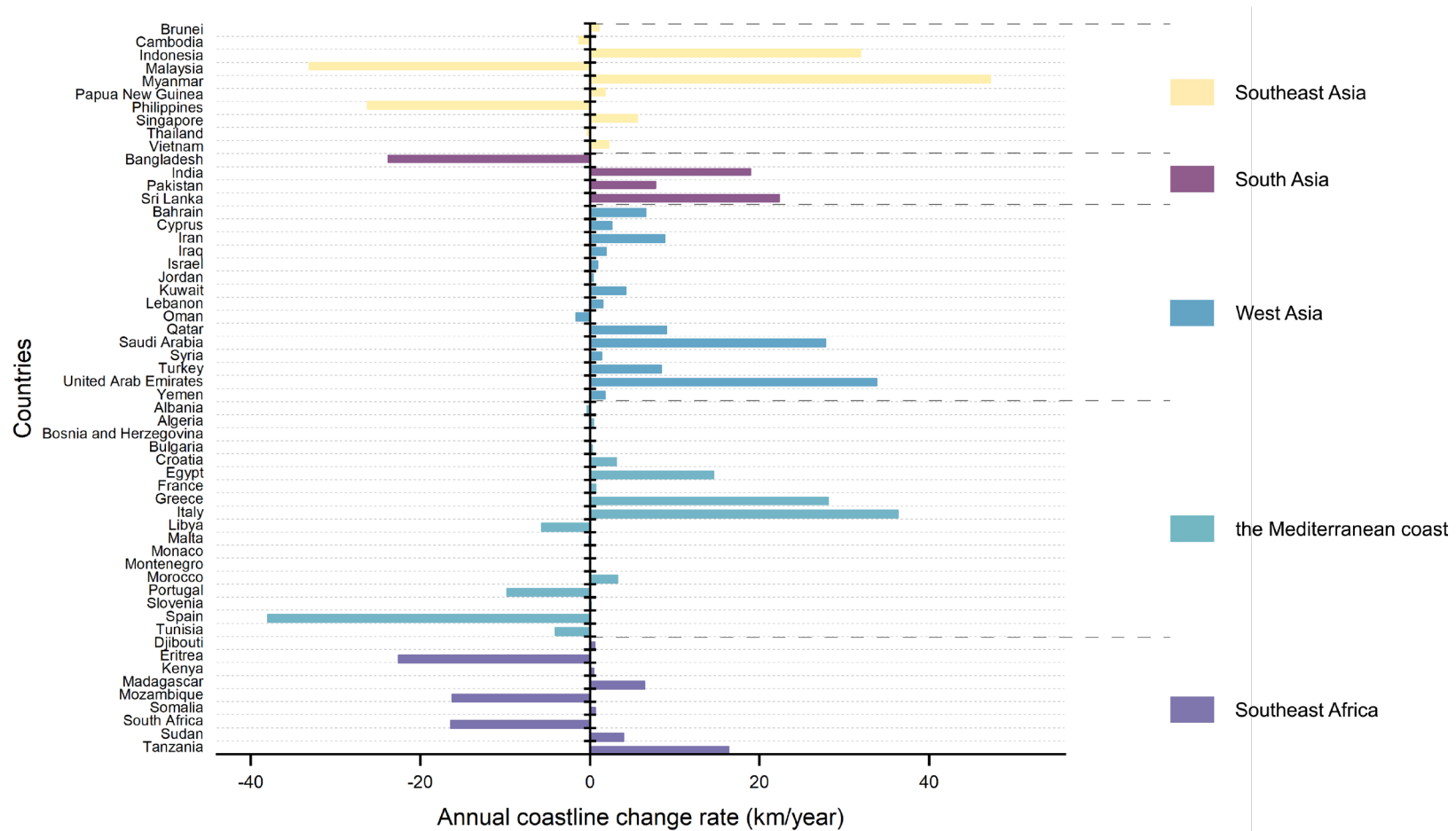


Figure 4. The annual change rate of coastline length for 56 countries from 1990 to 2020. We calculated the rate of coastline change over 30 years, and the values showed almost good normal distribution characteristics. Thus, we divided the rate of coastline change into four levels, arranging all values from smallest to largest and dividing them into quartiles, 0–25%, 25–50%, 50–75%, and 75–100%, and displayed them in the grids in Figure 5.

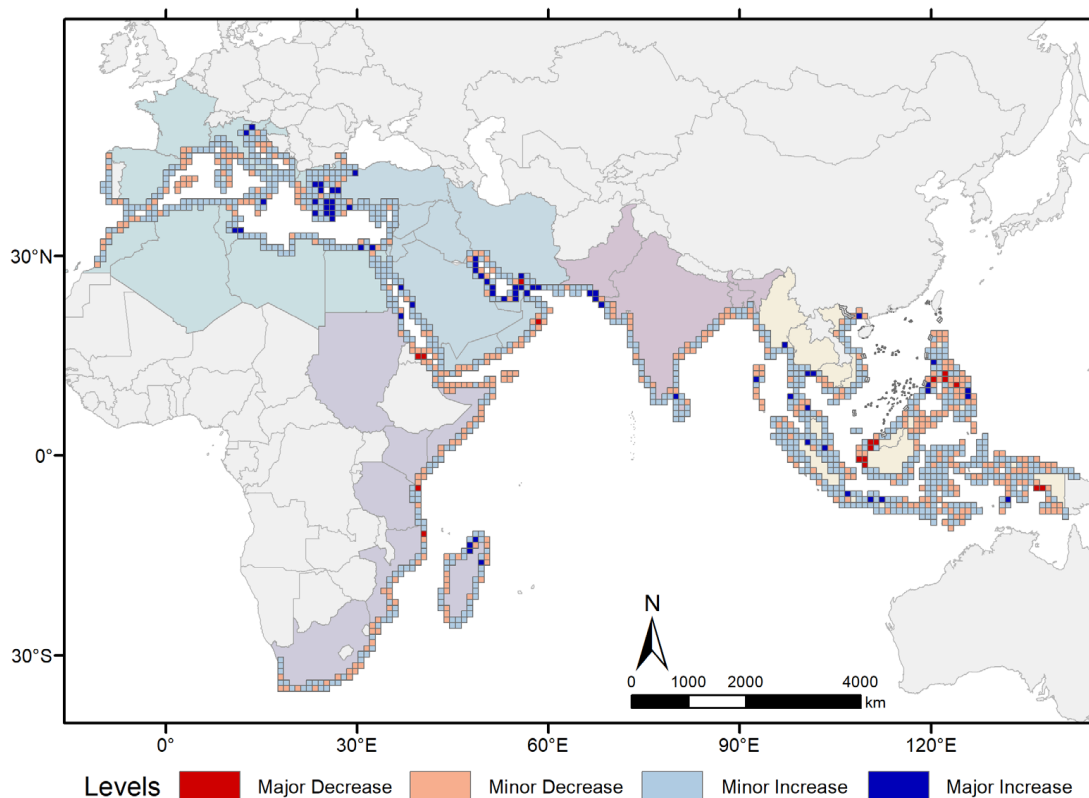


Figure 5. Grid distribution of coastline change rate in the 56 countries from 1990 to 2020. (The size of the grids: 100×100 m).

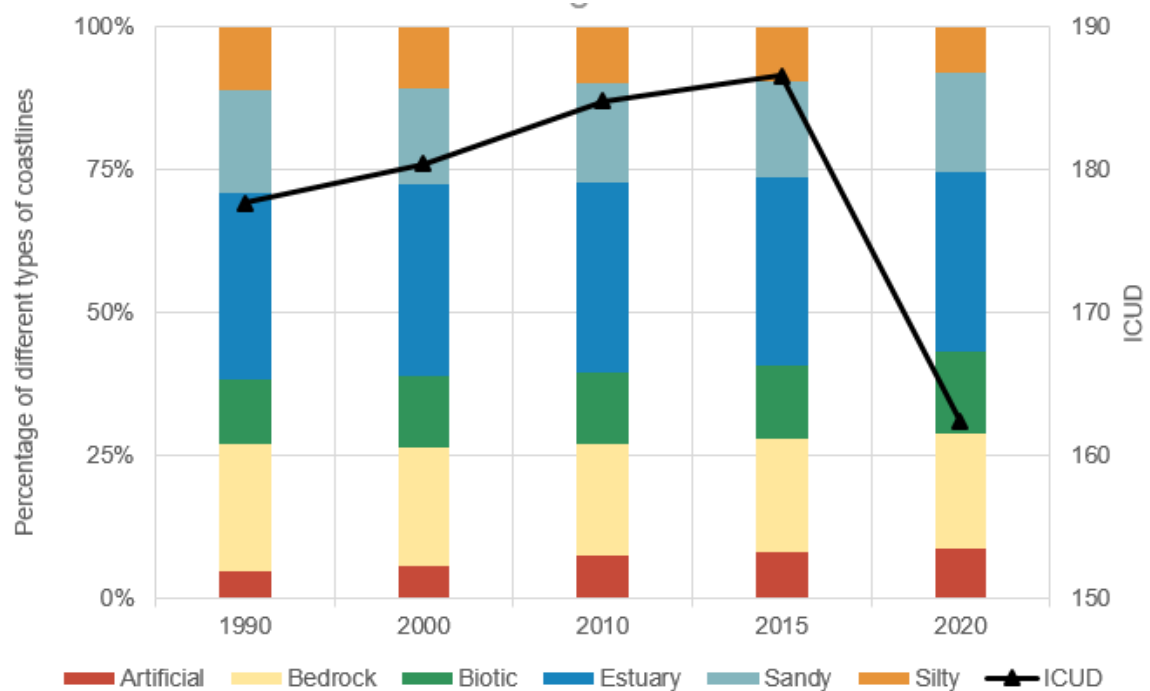
There has been an increasing trend along the coastlines of Southeast Asia, South Asia, West Asia, and the Mediterranean coast during the last 30 years. As shown in Figure 5, the coastline in Southeast Asia has grown more significant and extensive (light blue grid), increasing by approximately 860 km, with an annual rate of change of 28 km/year. The main increase in the coastline occurred along the northern coast of Indonesia (dark blue grid), and the decrease occurred in southwestern Malaysia and the Philippines (dark red grid). The coastline around South Asia has increased by about 756 km, with an annual rate of change of 25 km/year. The coastline in West Asia has increased more significantly (dark blue grid), increasing by approximately 3213 km, with an annual rate of change of 107 km/year. The coastline along the Mediterranean coast has increased by 863 km, with an annual rate of change of 29 km/year. The length of the coastline around Southeast Africa has fluctuated, with an overall decreasing trend, as shown in Figure 5 (light red grid), decreasing by about 1788 km over 30 years, with an annual rate of change of -59 km/year.

4.2. Coastline Structure Change

Coastline structure refers to the length proportion of different types of coastlines in a certain area, which can reflect the status of different types of coastlines under the influence of various activities. Therefore, we analyzed the coastline length proportion and annual change rate of various coastlines (Table 2 and Figure 6). The coastlines of the study area were mainly dominated by the estuary coastline, followed by bedrock coastline (Figure 6). Table 2 shows the rate of coastline change of different types from 1990 to 2020. The table shows that the total coastline change rates in 1990–2000, 2000–2010, 2010–2015, and 2015–2020 were 918.7, 537.1, -998.4 , and -1132.5 km/year, respectively.

Table 2. Length ratio and change rate of different coastlines types from 1990 to 2020.

Year		1990	2000	2010	2015	2020	
Natural coastline	Bedrock	Length ratio (%)	21.9%	20.7%	19.6%	19.5%	19.9%
		Change rate (km/year)		−238.9	−291.2	−227.3	21.8
	Biotic	Length ratio (%)	11.4%	12.3%	12.6%	12.9%	14.5%
		Change rate (km/year)		424.6	191.5	50.2	968.5
	Estuary	Length ratio (%)	32.8%	33.6%	33.3%	33.0%	31.4%
		Change rate (km/year)		577.7	54.5	−513.1	−1470.6
	Sandy	Length ratio (%)	17.9%	17.0%	17.2%	16.8%	17.4%
		Change rate (km/year)		−124.1	160.0	−442.2	186.2
	Silty	Length ratio (%)	11.1%	10.6%	9.9%	9.5%	8.0%
		Change rate (km/year)		−79.1	−202.9	−338.5	−1166.0
	Subtotal	Length ratio (%)	95.1%	94.2%	92.6%	91.8%	91.2%
		Change rate (km/year)		560.2	−88.0	−1471.0	−1459.9
	Artificial coastline	Length ratio (%)	4.9%	5.8%	7.4%	8.2%	8.8%
		Change rate (km/year)		358.4	625.1	472.6	327.4

**Figure 6.** Structural characters and index of coastline utilization degree (ICUD) of coastline from 1990–2020.

Regarding the natural coastline, the overall proportion of natural coastline length slowly decreased from 95.1% in the early 1990s to 91.2% in 2020. The length of the natural coastline increased slightly from 1990 to 2000, and since then, the length of the natural coastline decreased slowly, falling from 3.3×10^5 km in 2000 to 3.2×10^5 km in 2020.

The most obvious decrease in the natural coastline is the silty coastline, which has been decreasing from 3.8×10^4 km in 1990 to 2.8×10^4 km in 2020. Tidal scouring and

flooding will lead to a huge change in the silty coastline. In contrast, the bedrock coastline change rate shows an upward trend, and this means that the bedrock coastline is decreasing more and more slowly. Among the natural coastlines, almost all of them are decreasing in length percentage. Estuary and sandy coastline changed slightly, while estuary coastline decreased from 32.8% in 1990 to 31.4% in 2020, with a maximum dissolution rate of 1470.6 km/year between 2015 and 2020, and sandy coastline decreased from 17.9% in 1990 to 17.4% in 2020. Bedrock coastline decreased from 21.9% in 1990 to 19.9% in 2020, and silty coastline decreased from 11.1% in 1990 to 8.0% in 2020, reaching a maximum erosion rate of 1166.0 km/year between 2015 and 2020. In contrast, it is noteworthy that the biotic coastline length ratio has been consistently increasing from 11.4% in 1990 to 14.5% in 2020 and reaching an average annual growth rate of 968.5 km/year from 2015 to 2020. At the same time, the artificial coastline is growing rapidly, from 4.9% in 1990 to 8.8% in 2020. The average annual growth rate reached a maximum of 625.1 km/year in the period 2000–2010.

The ICUD index reflects the degree of influence of human activity on the coastline. Figure 6 shows a continuous increase in ICUD from 177.7 in 1990 to 186.6 in 2015, which shows that more and more coastlines were affected by human activities. However, it had a dramatic drop in 2020, reaching 162.5, implying that the coastlines became less affected by anthropogenic events, which corresponds with a significant increase in the biotic coastline between 2015 and 2020.

4.3. Coastline Fractal Dimension Change

The coastline fractal dimension (FD) provides an important precondition for accurate measurement of coastline length, promotion of intensive coastline use, and effective coastline protection and management. We calculated the fractal dimension of each country from 1990–2020. A series length of the grid (6000, 7000, 8000, 9000, 10,000, 11,000, 12,000, 13,000, and 14,000) were used to calculate the fractal dimension of the countries' coastlines. We found that most countries have a relatively stable trend of FD change, but a small number of countries have a large variation. The values of FD for five regions and for the countries with variable FD are shown in Figure 7a,b. Remote sensing images of some coastal zone areas with significant changes in FD are demonstrated (Figure 8).

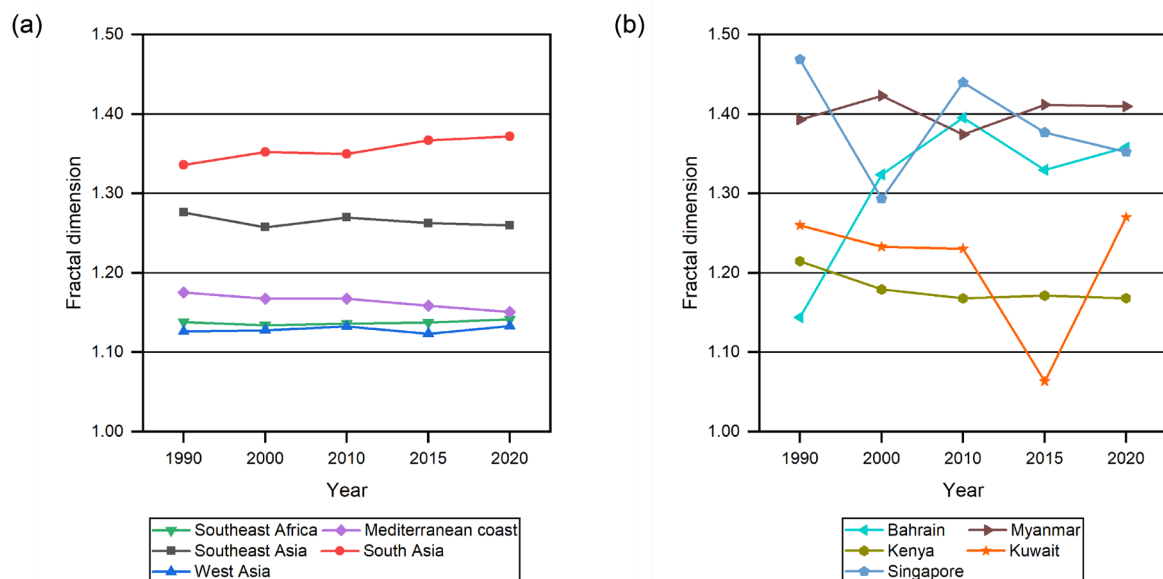


Figure 7. Fractal dimension (FD) of coastline in regions (a) and countries with highly variable FD (b).

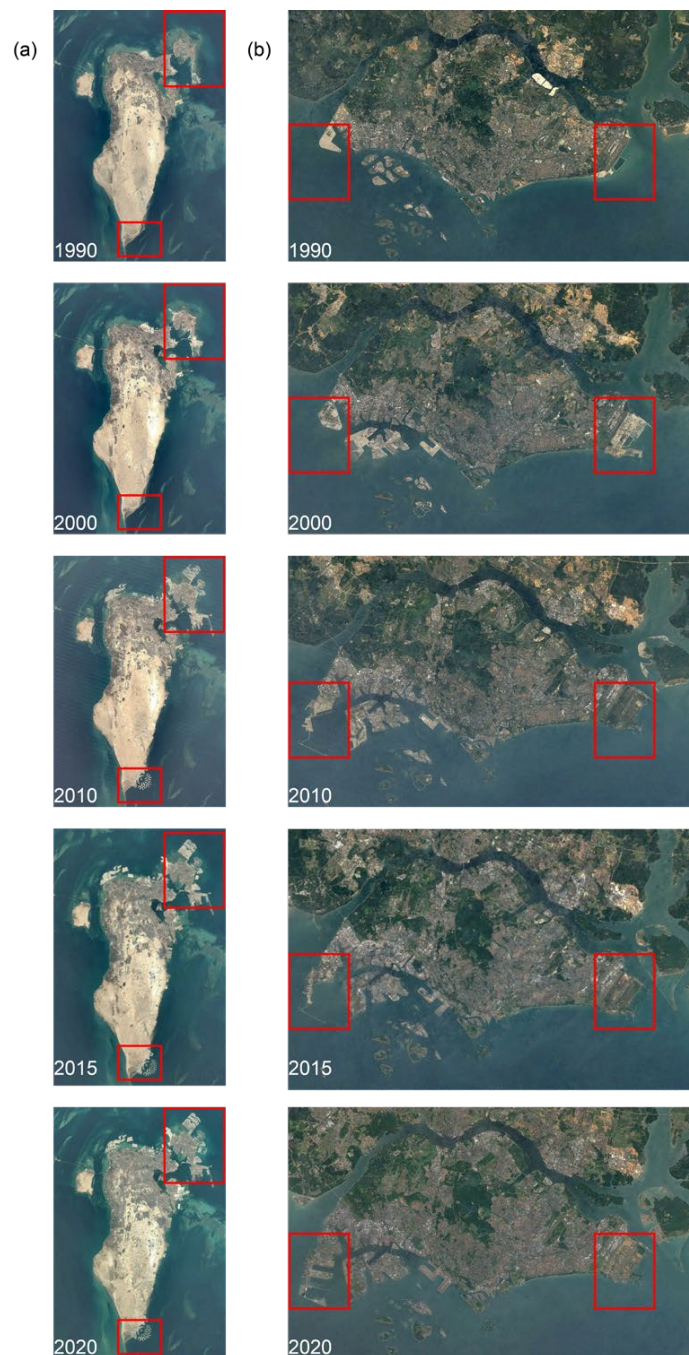


Figure 8. Landsat images of coastlines in the area with large fluctuations in FD values during 1990 and 2020: (a) the Bahrain coastal zone area, (b) the area along the Singapore coastal zone. Areas with great changes are circled in the red box.

At the regional scale (Figure 7a), South Asia had the highest FD values and has shown a gradual increase over the last 30 years. Southeast Asia was in second place but showed a slow decreasing trend. West Asia, the Mediterranean, and Southeast Africa had the lowest FD. The Mediterranean region was higher in terms of FD than Southeast Africa, while West Asia had the lowest FD. The FD of West Asia and Southeast Africa showed a slowly increasing trend, while the FD of the Mediterranean showed a more rapid decreasing trend. The larger the FD, the more curved and complex the coastline. This downward trend indicated that the coastline of Southeast Asia and the Mediterranean coast was more influenced by human activities, such as the building of dikes, the building of ports,

and reclamation, which make the originally curved coastline regular, thereby decreasing the FD.

In West Asia, Bahrain showed the highest average FD values, with a continuous increase from 1.14 to 1.40 between 1990 and 2010, and although its FD fluctuated between 2010 and 2020, it generally showed an increasing trend. As the remote sensing image in Figure 8 shows, the coastlines of Bahrain became more curved and thus complex from 1990 to 2020. It can be clearly seen that many artificial structures, such as docks and harbors, have been built around this coastal zone, so the FD value shows an increasing trend. In Southeast Asia, the FD value of Singapore decreased from 1.47 to 1.29, followed by an increase between 1990 and 2010 and a slight decrease after 2010, which indicated that the shape of the coastline along Singapore had undergone major changes during this period (Figure 8). The FD value of Slovenia in the Mediterranean Sea showed a continuous decreasing trend from 1.50 to 0.88 during the period 1990–2020. Similarly, in Kuwait, the frequent shipping in the port made the coastline more and more tortuous, which led to the coastline being more curved and its FD value changing. The FD value of Kuwait fell from 1.23 to 1.06 from 2010 to 2015 but increased to 1.27 in 2020.

4.4. Changes of Land-Sea Pattern

Changes in coastline erosion or accretion caused by human activities (land reclamation and development) or natural changes (tides, sedimentation) are expressed at a macro level as changes in the advance and retreat between sea and land. Changes in land-sea patterns respond to the direction and process of coastline erosion or expansion, and changes in coastline structure types explain the main drivers and factors of changes in land-sea patterns. By comparing the coastline changes between the two periods, the sea-land pattern could reflect the changes in the coastal zone area.

From 1990 to 2020, the coastal areas of Eurasia and Africa changed dramatically, with land expansion of about 9663.15 km² and land retreat of about 5913.75 km². It showed that the trend of the coastline change was mainly expansion into the sea (land advancing and coastline expansion), and there was relatively less erosion to land (land retreating and coastline erosion) (Figure 9a).

The areas with large changes in land-sea patterns are mainly distributed in South Asia and Southeast Asia. Most of the countries in Southeast Asia showed a net increase in land area in coastal areas. Indonesia, the Philippines, and Vietnam showed a land advance with a net increase of about 2223.88 km², 863.22 km², and 419.42 km² (Figure 9b). In South Asia, Bangladesh showed a net increase in land area of 222.49 km², India showed a retreat of land area with a net change of −512.61 km², and Pakistan had a significant change of the land area of about −561.71 km² (Figure 9c). Many countries in Southeast Africa maintained a slight change in coastline area, showing a slight erosion (Figure 9d). Among the Mediterranean coastal countries, Egypt and Greece suffered coastal erosion, with land retreating of area change of −23.28 km² and −11.74 km², respectively (Figure 9e). Most countries in West Asia remained a net increase in land area, with Iran showing the largest increase of area of about 292.29 km² and Turkey of about 196.44 km² (Figure 9f).

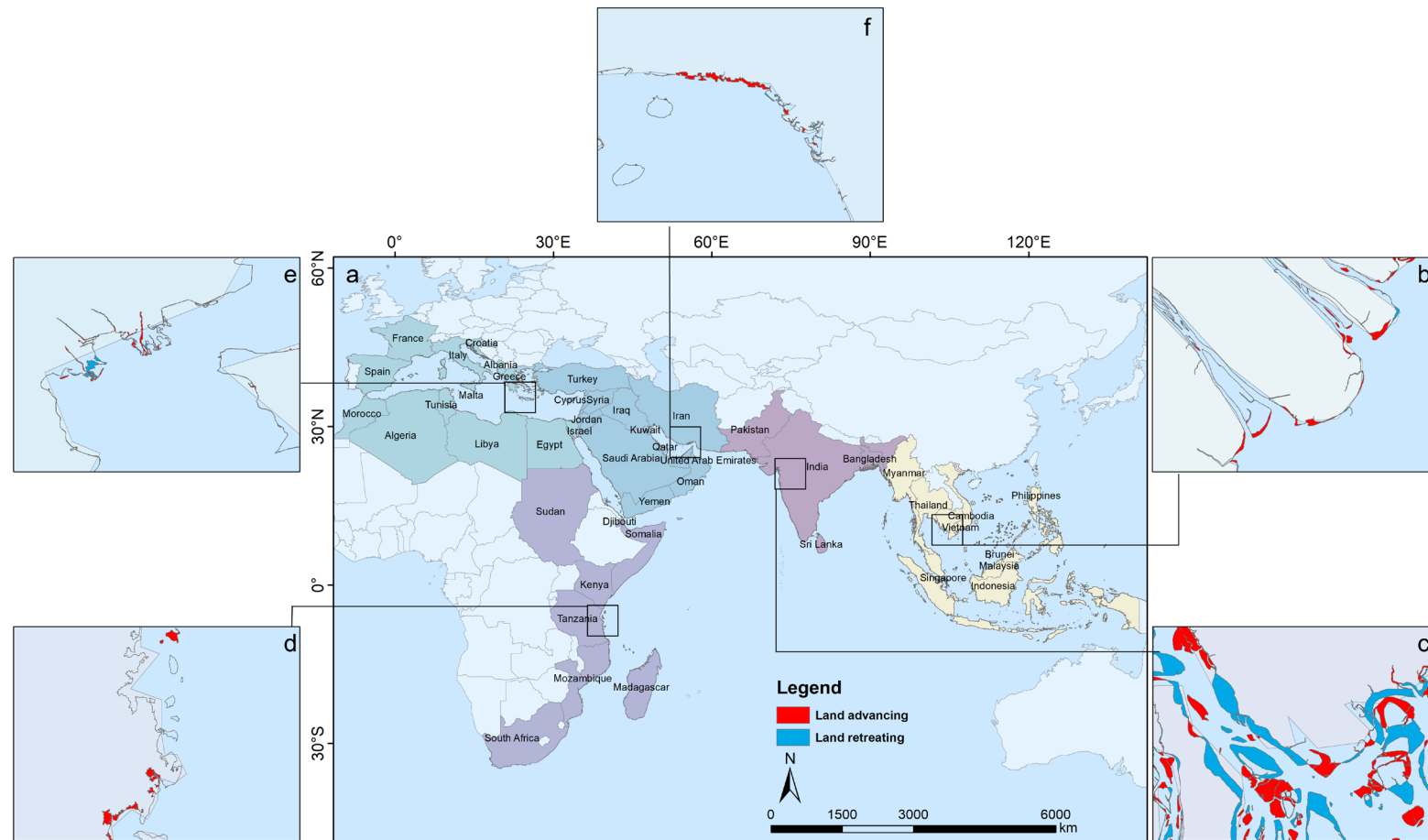


Figure 9. Spatial distribution for land-sea pattern in Eurasia and African continents (colored as Figure 1): (a), Vietnam, Southeast Asia (b), India, South Asia (c), Tanzania, Southeast Africa (d), Greece, the Mediterranean coast (e), and Iran, West Asia (f) from 1990 to 2020.

5. Discussion

5.1. Driving Factors and Potential Impacts for Coastline Change

The coast is a very important buffer zone between the land and sea, which provides services including carbon storage, protection for coastal settlements, and a balanced environment for ocean life [49]. Based on the previous research [8,9], in the past 30 years, the continuous expansion of human activities has led to effects on the coastline, therefore, the original structure of the coastline has been affected. Specifically, the length of the entire coastline showed a decreasing trend after 2010, indicating that the coastline is suffering severe disturbances.

Based on the changes in various types of coastlines from 1990 to 2020 (Figure 6), especially the continuous growth of artificial coastlines, it can be inferred that human activities are the main drivers of coastline change. Geographically, Southeast and South Asia are the main regions contributing to the overall growth of artificial coastline length [50], as most developing countries are experiencing rapid development of their marine economies, with coastal countries such as Indonesia and Myanmar vigorously developing their aquaculture industries and accelerating the rate of expansion of aquaculture ponds [51]. The reduction of coastline is mainly concentrated in Eritrea, Mozambique, and South Africa in Southeast Africa, where marine economic development is relatively weak. Coral bleaching and some aquaculture ponds are frequently affected by coastline erosion, monsoonal winds, and sea level rise, which results in an overall decreasing trend in coastline length [52].

In terms of coastline type, although the proportion of artificial coastline is low, it is widely distributed and is the main driver of overall coastline length growth. Artificial coastlines are mainly densely distributed along the Mediterranean coast, the Persian Gulf coast in West Asia, the Strait of Malacca, the Red Sea coast, and the northern part of Java Island in Southeast Asia, which consists of breeding ponds, port towns, cargo ports, and reclamation projects that carry great economic significance [53]. Urban development of ports and coastal zones, human activities, and marine economic construction are the main drivers of the growth of artificial coastlines, such as the construction of coastal farming ponds in Southeast Asian countries, the upgrading and expansion of ports in various countries, reclamation projects in island countries, and intensive touristic activities in West Asia [54]. Compared to other studies, our results of the Index of Coastline Utilization Degree (ICUD) data further illustrate the driving factors of coastline changes. In general, the ICUD of the coastline across the study area increased almost continuously until 2015, with a large and rapid increase between 2000 and 2010, a period when the growth rate of the artificial coastline also reached its maximum and the intensity of human activities on the coastline continued to increase.

The natural coastline retention rate refers to the ratio of the retained length of the mainland natural coastline to the total length of the mainland coastline. Setting this indicator is conducive to strengthening coastline protection, utilization, management, and improving marine ecology. From 1990 to 2020, the natural coastline retention rate along the seashore declined from 95.1% to 91.2%. When we compare the changes in the length of different types of coastlines, we can figure out the differences and changes in the structure of the coastlines. The proportions of biotic coastline and artificial coastline are increasing continuously, and the proportion of silty coastline is decreasing significantly. More and more countries are paying more attention to environmental protection and biodiversity. Coastal zone areas, such as coral reefs, mangroves, and coastal wetlands, have been protected and developed, increasing the biotic coastline percentage [55,56]. The biotic coastline is mainly dominated by mangroves and other offshore plants, concentrated in Southeast Asia, which increased from 3.9 km (1990) to 5.1 km (2020). Mangrove forests are an effective barrier to the coast, and proper planting and protection will mitigate the effects of climate change in coastal regions [57,58].

The Sustainable Development Goals (SDGs) are a set of global goals set by the United Nations in 2015 to achieve a better and more sustainable future for the public, with 17 goals accompanied by 169 specific targets. SDG 14 emphasizes the protection and sustainable

development of oceans and marine resources, and SDG 14.5 addresses the protection of coastal and marine areas, suggesting that, by 2020, our world should protect at least 10% of coastal and marine areas with national and international law. The impact of the intensity of human activities on the coastline has been dramatically reduced, as can also be seen in Figure 6, where the ICUD shows a decreasing trend after 2015.

5.2. Selected Regions for Detailed Analysis

Changes in coastline structure can be closely related to the direction of a country's marine economic development, as well as resource development and utilization [59]. Many previous studies have investigated changes in coastline length, but most of them only focused on individual countries or regions [33,44]. In terms of changes in coastline length, considering the coastline changes of the countries over the past 30 years, Southeast Africa frequently suffered natural disasters such as tsunamis and hurricanes [52], and the coastline length in this region continued to decrease. Owing to busy maritime trade and developed tourism, the Red Sea and the Mediterranean Sea along the route are the regions with a concentrated coastline increase (Figure 5).

Focusing on the coastline structure change, it is evident that countries with a large proportion of artificial coastlines are mainly those with developing aquaculture and are rich in marine resources. The coastline changes in the Southeast Asia region are mainly based on the artificial coastline, which is manifested by the phenomena of aquaculture ponds, dykes, and polders. This is inseparably related to the developed local aquaculture industry. The countries with a large proportion of bedrock coastline, on the other hand, have natural geographical advantages at the hub of seas, such as the Black Sea and the Red Sea, and have more natural resources, such as oil, so their marine trade mainly relies on ocean import and export of resources [60]. Countries near West Asia and the Mediterranean Sea are located at the center of the oceans and straits and have rich oil and gas resources, so they rely mainly on marine imports and export to drive the development of the maritime economy. In addition, for the natural-disaster-prone Southeast of Africa, Madagascar's coastline shows fluctuating changes in silty and sandy coastlines, whereas Southeast Africa shows sandy coastline increasing and estuary coastline decreasing.

The eroded coastline is mainly estuary and silty coastlines. It has been shown that the natural coastline of Indonesia has been reduced by about 6000 km in the last 30 years [61]. The coastline in Southeast Asia is long and rich in types. According to our analysis of coastline types, we found that most of the Indonesian coast is silty coast. The erosion of the silty coast is mainly due to wave and tidal action in seawater and the scouring action of rivers, which leads to the retreat and erosion of the coastline. The Estuary coastline in South Asia is generally subject to significant erosion, and the coastline with the fastest erosion rate is along Bangladesh. Bangladesh is a country bordering the sea, with a coastline that spans the southern coast of the country that is also connected to the Bay of Bengal. The erosion of Bangladesh's estuary coastline is mainly due to precipitation from monsoons, combined with the low and flat topography of Bangladesh, slow-flowing rivers, severe siltation of rivers, and estuarine displacements [62], resulting in flooding, siltation of rivers, and severe displacement and erosion of the estuary coastline.

It is estimated that about 3 million hectares of global mangrove area were lost between 1980 and 2005, the largest proportion in Southeast Asia, where about 50% of the mangroves were lost; the area from which mangroves were lost was mainly converted to aquaculture or agriculture, and the others were lost due to urban development [63–65]. The reduction in the biotic coastline is concentrated in some countries in Southeast Asia. Large aquaculture countries, such as Thailand and Myanmar, need to balance their aquaculture and coastal zone area conservation. Few studies have used fractal dimensional to estimate coastline change. As with the FD values calculated in this study, the West Asia region has the lowest average FD in almost all study areas. When combined with Figure 7, it is obvious that the coastal zone areas in West Asia, on the other hand, are mainly used for port expansion and maritime trade; these activities are prone to sediment accumulation and tides, which

threaten urban life, so a balance should also be established between economic development brought about by artificial coastlines and comfortable living space for humans [66]. A series of serious problems, such as sea level rise, seawater flooding, dike construction, cyclones, and the degradation of mangroves are problems that need to be solved to protect the coastal zone area [67], and we still need a lot of effort to solve these issues and conserve the coastal zone.

6. Conclusions

In this study, the spatial locations and types of 56 coastal countries' coastlines and their change patterns over the past 30 years (1990–2020) were mapped using Landsat time series. Significant coastline changes occurred during the study period. From 1990 to 2020, the coastline of 56 coastal countries increased from 3.45×10^5 km to 3.59×10^5 km. The length ratio of artificial coastline rose from 4.9% to 8.8%, while the proportion of natural coastline fell from 95.1% to 91.2%. Coastal spreading is a prevalent trend observed on most coastlines. In particular, the majority of coastlines in Southeast and West Asia exhibit spreading. Conversely, South Asian coastlines predominantly experience erosion. Minor erosion is also observed in coastlines along southeastern Africa and the Mediterranean Sea. Between 2000 and 2010, the coastline underwent a significant process of curvature change and complexity change, especially in some countries in Southeast Asia and West Asia, such as Singapore, Myanmar, Brunei, Bahrain, and Vietnam. During this period, human activities have had a significant impact on the spatial and temporal variability of the coastline [65]. Most of the coastlines are being eroded, with severe erosion of silty coastline in Southeast Asia and estuarine coastline in South Asia. Biotic coastlines are effectively protected, and areas containing mangroves and coral reefs in Southeast Asia show a growing trend.

Changes in coastlines are closely related to the development of the marine economy in the region, and thriving coastal zone development can significantly boost regional economic development. We should seek a balance between economic development and coastal zone protection. Since the first year of the Sustainable Development Goals (2015), the growth in the length of the coastline and artificial coastline has started to slow down, indicating that coastal countries have achieved some success in the scientific management and planning of coastlines. Highly efficient and accurate research methods should be used to further study and protect coastlines. In the future, we will investigate the precise coastline erosion or accretion state on a large spatial scale, which can provide data support for understanding the spatial and temporal changes in coastal countries' coastlines and support decision-making in the land-use planning and sustainable development in coastal areas.

Author Contributions: F.Y. and B.C. were responsible for conducting the experiment and data analysis. L.Z. designed the concept and the methodology of the study and revised the manuscript. J.L. and K.L. collected and processed the image data. R.M., M.E.H., M.M.A.A.M., S.A.R. and D.S. helped with the analysis and reviewed the manuscript. All authors have read and agreed to the published version of the manuscript.

Funding: The authors are grateful for the support from the Strategic Priority Research Program of the Chinese Academy of Sciences (Grant No. XDA19030302) and National Natural Science Foundation of China (Grant No. 42071305).

Data Availability Statement: The data presented in this study are available on request from the corresponding authors (B.C. and L.Z.).

Acknowledgments: We would like to acknowledge these colleagues who assisted with the coastline extraction surveys and information collection and would like to specifically thank the nameless reviewers for their voluntary work and the positive feedback to enhance this manuscript.

Conflicts of Interest: The authors declare no conflict of interest.

References

- Fabinyi, M.; Belton, B.; Dressler, W.H.; Knudsen, M.; Adhuri, D.S.; Abdul Aziz, A.; Akber, M.A.; Kittitornkool, J.; Kongkaew, C.; Marschke, M.; et al. Coastal Transitions: Small-Scale Fisheries, Livelihoods, and Maritime Zone Developments in Southeast Asia. *J. Rural Stud.* **2022**, *91*, 184–194. [\[CrossRef\]](#)
- Žilinskas, G.; Janušaitė, R.; Jarmalavičius, D.; Pupienis, D. The Impact of Klaipėda Port Entrance Channel Dredging on the Dynamics of Coastal Zone, Lithuania. *Oceanologia* **2020**, *62*, 489–500. [\[CrossRef\]](#)
- Romine, B.M.; Fletcher, C.H. A Summary of Historical Shoreline Changes on Beaches of Kauai, Oahu, and Maui, Hawaii. *J. Coast. Res.* **2013**, *288*, 605–614. [\[CrossRef\]](#)
- Krien, Y.; Dudon, B.; Roger, J.; Arnaud, G.; Zahibo, N. Assessing Storm Surge Hazard and Impact of Sea Level Rise in the Lesser Antilles Case Study of Martinique. *Nat. Hazards Earth Syst. Sci.* **2017**, *17*, 1559–1571. [\[CrossRef\]](#)
- Hou, J.; Li, X.; Wang, P.; Wang, J.; Ren, Z. Hazard Analysis of Tsunami Disaster on the Maritime Silk Road. *Acta Oceanol. Sin.* **2020**, *39*, 74–82. [\[CrossRef\]](#)
- Aiello, A.; Canora, F.; Pasquariello, G.; Spilotro, G. Shoreline Variations and Coastal Dynamics: A Space-Time Data Analysis of the Jonian Littoral, Italy. *Estuar. Coast. Shelf Sci.* **2013**, *129*, 124–135. [\[CrossRef\]](#)
- Thia-Eng, C. Essential Elements of Integrated Coastal Zone Management. *Ocean Coast. Manag.* **1993**, *21*, 81–108. [\[CrossRef\]](#)
- Small, C.; Nicholls, R.J. A Global Analysis of Human Settlement in Coastal Zones. *J. Coast. Res.* **2003**, *19*, 584–599.
- Kummu, M.; de Moel, H.; Salvucci, G.; Viviroli, D.; Ward, P.J.; Varis, O. Over the Hills and Further Away from Coast: Global Geospatial Patterns of Human and Environment over the 20th–21st Centuries. *Environ. Res. Lett.* **2016**, *11*, 034010. [\[CrossRef\]](#)
- Kannan, R.; Anand, K.V.; Sundar, V.; Sannasiraj, S.A.; Rangarao, V. Shoreline Changes along the Northern Coast of Chennai Port, from Field Measurements. *ISH J. Hydraul. Eng.* **2014**, *20*, 24–31. [\[CrossRef\]](#)
- Petrișor, A.-I.; Hamma, W.; Nguyen, H.D.; Randazzo, G.; Muzirafuti, A.; Stan, M.-I.; Tran, V.T.; Aștefănoaiei, R.; Bui, Q.-T.; Vintilă, D.-F.; et al. Degradation of Coastlines under the Pressure of Urbanization and Tourism: Evidence on the Change of Land Systems from Europe, Asia and Africa. *Land* **2020**, *9*, 275. [\[CrossRef\]](#)
- Nicholls, R.J.; Woodroffe, C.; Burkett, V. Chapter 20—Coastline Degradation as an Indicator of Global Change. In *Climate Change*, 2nd ed.; Letcher, T.M., Ed.; Elsevier: Boston, MA, USA, 2016; pp. 309–324.
- Hegazy, I.R. Towards Sustainable Urbanization of Coastal Cities: The Case of Al-Arish City, Egypt. *Ain Shams Eng. J.* **2021**, *12*, 2275–2284. [\[CrossRef\]](#)
- Luijendijk, A.; Hagenaars, G.; Ranasinghe, R.; Baart, F.; Donchyts, G.; Aarninkhof, S. The State of the World's Beaches. *Sci. Rep.* **2018**, *8*, 6641. [\[CrossRef\]](#) [\[PubMed\]](#)
- Pajak, M.J.; Leatherman, S. The High Water Line as Shoreline Indicator. *J. Coast. Res.* **2002**, *18*, 329–337.
- Kabir, M.A.; Salaudhin, M.; Hossain, K.T.; Tanim, I.A.; Saddam, M.M.H.; Ahmad, A.U. Assessing the Shoreline Dynamics of Hatiya Island of Meghna Estuary in Bangladesh Using Multiband Satellite Imageries and Hydro-Meteorological Data. *Reg. Stud. Mar. Sci.* **2020**, *35*, 101167. [\[CrossRef\]](#)
- Mills, J.P.; Buckley, S.J.; Mitchell, H.L.; Clarke, P.J.; Edwards, S.J. A Geomatics Data Integration Technique for Coastal Change Monitoring. *Earth Surf. Process. Landf.* **2005**, *30*, 651–664. [\[CrossRef\]](#)
- Xu, N. Detecting Coastline Change with All Available Landsat Data over 1986–2015: A Case Study for the State of Texas, USA. *Atmosphere* **2018**, *9*, 107. [\[CrossRef\]](#)
- Masselink, G.; Brooks, S.; Poate, T.; Stokes, C.; Scott, T. Coastal Dune Dynamics in Embayed Settings with Sea-Level Rise—Examples from the Exposed and Macrotidal North Coast of SW England. *Mar. Geol.* **2022**, *450*, 106853. [\[CrossRef\]](#)
- Murray, N.J.; Phinn, S.P.; Fuller, R.A.; DeWitt, M.; Ferrari, R.; Johnston, R.; Clinton, N.; Lyons, M.B. High-resolution global maps of tidal flat ecosystems from 1984 to 2019. *Sci. Data* **2022**, *9*, 542. [\[CrossRef\]](#)
- Jennings, S. Coastal Tourism and Shoreline Management. *Ann. Tour. Res.* **2004**, *31*, 899–922. [\[CrossRef\]](#)
- Peterson, C.H.; Bishop, M.J. Assessing the Environmental Impacts of Beach Nourishment. *BioScience* **2005**, *55*, 887. [\[CrossRef\]](#)
- Syvitski, J.P.M.; Kettner, A.J.; Overeem, I.; Hutton, E.W.H.; Hannon, M.T.; Brakenridge, G.R.; Day, J.; Vörösmarty, C.; Saito, Y.; Giosan, L.; et al. Sinking Deltas Due to Human Activities. *Nat. Geosci.* **2009**, *2*, 681–686. [\[CrossRef\]](#)
- Carugati, L.; Gatto, B.; Rastelli, E.; Lo Martire, M.; Coral, C.; Greco, S.; Danovaro, R. Impact of Mangrove Forests Degradation on Biodiversity and Ecosystem Functioning. *Sci. Rep.* **2018**, *8*, 13298. [\[CrossRef\]](#) [\[PubMed\]](#)
- Cao, T.; Han, D.; Song, X. Past, Present, and Future of Global Seawater Intrusion Research: A Bibliometric Analysis. *J. Hydrol.* **2021**, *603*, 126844. [\[CrossRef\]](#)
- Janušaitė, R.; Jarmalavičius, D.; Pupienis, D.; Žilinskas, G.; Jukna, L. Nearshore Sandbar Switching Episodes and Their Relationship with Coastal Erosion at the Curonian Spit, Baltic Sea. *Oceanologia* **2021**, *65*, S007832342100097X. [\[CrossRef\]](#)
- Phan, M.H.; Stive, M.J.F. Managing Mangroves and Coastal Land Cover in the Mekong Delta. *Ocean Coast. Manag.* **2022**, *219*, 106013. [\[CrossRef\]](#)
- Dar, I.A.; Dar, M.A. Prediction of Shoreline Recession Using Geospatial Technology: A Case Study of Chennai Coast, Tamil Nadu, India. *J. Coast. Res.* **2009**, *256*, 1276–1286. [\[CrossRef\]](#)
- Ng, L.S.; Campos-Arceiz, A.; Sloan, S.; Hughes, A.C.; Tiang, D.C.F.; Li, B.V.; Lechner, A.M. The Scale of Biodiversity Impacts of the Belt and Road Initiative in Southeast Asia. *Biol. Conserv.* **2020**, *248*, 108691. [\[CrossRef\]](#)
- Hughes, A.C.; Lechner, A.M.; Chitov, A.; Horstmann, A.; Hinsley, A.; Tritto, A.; Chariton, A.; Li, B.V.; Ganapin, D.; Simonov, E.; et al. Horizon Scan of the Belt and Road Initiative. *Trends Ecol. Evol.* **2020**, *35*, 583–593. [\[CrossRef\]](#)

31. Li, S.; Liu, Y.; Yang, H.; Yu, X.; Zhang, Y.; Wang, C. Integrating Ecosystem Services Modeling into Effectiveness Assessment of National Protected Areas in a Typical Arid Region in China. *J. Environ. Manag.* **2021**, *297*, 113408. [\[CrossRef\]](#)
32. Liu, Q.; Trinder, J.; Turner, I.L. Automatic Super-Resolution Shoreline Change Monitoring Using Landsat Archival Data: A Case Study at Narrabeen-Collaroy Beach, Australia. *J. Appl. Remote Sens.* **2017**, *11*, 016036. [\[CrossRef\]](#)
33. Muttitanon, W.; Tripathi, N.K. Land Use/Land Cover Changes in the Coastal Zone of Ban Don Bay, Thailand Using Landsat 5 TM Data. *Int. J. Remote Sens.* **2005**, *26*, 2311–2323. [\[CrossRef\]](#)
34. Shalaby, A.; Tateishi, R. Remote Sensing and GIS for Mapping and Monitoring Land Cover and Land-Use Changes in the Northwestern Coastal Zone of Egypt. *Appl. Geogr.* **2007**, *27*, 28–41. [\[CrossRef\]](#)
35. Zheng, C.W.; Pan, J.; Li, C.Y. Global Oceanic Wind Speed Trends. *Ocean Coast. Manag.* **2016**, *129*, 15–24. [\[CrossRef\]](#)
36. Boak, E.H.; Turner, I.L. Shoreline definition and detection: A review. *J. Coast. Res.* **2005**, *21*, 688–703. [\[CrossRef\]](#)
37. McAllister, E.; Payo, A.; Novellino, A.; Dolphin, T.; Medina-Lopez, E. Multispectral satellite imagery and machine learning for the extraction of shoreline indicators. *Coast. Eng.* **2022**, *174*, 104102. [\[CrossRef\]](#)
38. Cadier, C.; Bayraktarov, E.; Piccolo, R.; Adame, M.F. Indicators of Coastal Wetlands Restoration Success: A Systematic Review. *Front. Mar. Sci.* **2020**, *7*, 600220. [\[CrossRef\]](#)
39. Yasir, M.; Sheng, H.; Fan, H.; Nazir, S.; Niang, A.J.; Salauddin, M.; Khan, S. Automatic Coastline Extraction and Changes Analysis Using Remote Sensing and GIS Technology. *IEEE Access* **2020**, *8*, 180156–180170. [\[CrossRef\]](#)
40. Iqbal, M.A.; Anghel, A.; Datcu, M. Coastline Extraction From SAR Data Using Doppler Centroid Images. *IEEE Geosci. Remote Sensing Lett.* **2022**, *19*, 1506205. [\[CrossRef\]](#)
41. Gens, R. Remote Sensing of Coastlines: Detection, Extraction and Monitoring. *Int. J. Remote Sens.* **2010**, *31*, 1819–1836. [\[CrossRef\]](#)
42. Suo, A.N.; Cao, K.; Ma, H.W.; Wang, Q.M.; Yu, Y.H. Discussion on Classification System of Coastline. *Sci. Geogr. Sin.* **2015**, *35*, 933–937. (In Chinese)
43. Kuleli, T.; Guneroglu, A.; Karsli, F.; Dihkan, M. Automatic Detection of Shoreline Change on Coastal Ramsar Wetlands of Turkey. *Ocean Eng.* **2011**, *38*, 1141–1149. [\[CrossRef\]](#)
44. Wu, T. *Analysis of Spatio-Temporal Characteristics of Mainland Coastline Changes in China in Nearly 70 Years*; Yantai Institute of Coastal Zone Research, Chinese Academy of Sciences: Yantai, China, 2016. (In Chinese)
45. Zhuang, D.F.; Liu, J.Y. Study on the Model of Regional Differentiation of Land Use Degree in China. *J. Nat. Resour.* **1997**, *12*, 10–16. (In Chinese)
46. Husain, A.; Reddy, J.; Bisht, D.; Sajid, M. Fractal Dimension of India Using Multicore Parallel Processing. *Comput. Geosci.* **2022**, *159*, 104989. [\[CrossRef\]](#)
47. Bowers, D.G.; McKee, D.; Jago, C.F.; Nimmo-Smith, W.A.M. The Area-to-Mass Ratio and Fractal Dimension of Marine Flocs. *Estuar. Coast. Shelf Sci.* **2017**, *189*, 224–234. [\[CrossRef\]](#)
48. Liebovitch, L.S.; Toth, T. A Fast Algorithm to Determine Fractal Dimensions by Box Counting. *Phys. Lett. A* **1989**, *141*, 386–390. [\[CrossRef\]](#)
49. Kirwan, M.L.; Megonigal, J.P. Tidal Wetland Stability in the Face of Human Impacts and Sea-Level Rise. *Nature* **2013**, *504*, 53–60. [\[CrossRef\]](#)
50. Fisheries, F.A.O. *The State of World Fisheries and Aquaculture*; Food and Agriculture Organization of the United Nations: Rome, Italy, 2019.
51. Rimmer, M.A.; Sugama, K.; Rakhmawati, D.; Rofiq, R.; Habgood, R.H. A Review and SWOT Analysis of Aquaculture Development in Indonesia. *Rev. Aquac.* **2013**, *5*, 255–279. [\[CrossRef\]](#)
52. Jacobs, Z.L.; Yool, A.; Jebri, F.; Srokosz, M.; van Gennip, S.; Kelly, S.J.; Roberts, M.; Sauer, W.; Queirós, A.M.; Osuka, K.E.; et al. Key Climate Change Stressors of Marine Ecosystems along the Path of the East African Coastal Current. *Ocean Coast. Manag.* **2021**, *208*, 105627. [\[CrossRef\]](#)
53. Dastgheib, A.; Reyms, J.; Thammasittirong, S.; Weesakul, S.; Thatcher, M.; Ranasinghe, R. Variations in the Wave Climate and Sediment Transport Due to Climate Change along the Coast of Vietnam. *J. Mar. Sci. Eng.* **2016**, *4*, 86. [\[CrossRef\]](#)
54. Awad, M.; El-Sayed, H.M. The Analysis of Shoreline Change Dynamics and Future Predictions Using Automated Spatial Techniques: Case of El-Omayed on the Mediterranean Coast of Egypt. *Ocean Coast. Manag.* **2021**, *205*, 105568. [\[CrossRef\]](#)
55. Wang, J.; Chen, J.; Wen, Y.; Fan, W.; Liu, Q.; Tarolli, P. Monitoring the Coastal Wetlands Dynamics in Northeast Italy from 1984 to 2016. *Ecol. Indic.* **2021**, *129*, 107906. [\[CrossRef\]](#)
56. Chamberland-Fontaine, S.; Thomas Estrada, G.; Heckadon-Moreno, S.; Hickey, G.M. Enhancing the Sustainable Management of Mangrove Forests: The Case of Punta Galeta, Panama. *Trees For. People* **2022**, *8*, 100274. [\[CrossRef\]](#)
57. Kozhikkodan Veetil, B.; Quang, N.X. Mangrove Forests of Cambodia: Recent Changes and Future Threats. *Ocean Coast. Manag.* **2019**, *181*, 104895. [\[CrossRef\]](#)
58. Guo, Y.; Liao, J.; Shen, G. Mapping Large-Scale Mangroves along the Maritime Silk Road from 1990 to 2015 Using a Novel Deep Learning Model and Landsat Data. *Remote Sens.* **2021**, *13*, 245. [\[CrossRef\]](#)
59. Gai, M.; Zhan, Y. Spatial Evolution of Marine Ecological Efficiency and Its Influential Factors in China Coastal Regions. *Sci. Geogr. Sin.* **2019**, *39*, 616–625.
60. Kong, H.; Shen, L.; Zhong, S. Dynamic Relations among Oil Production and Trade and Economic Growth in Oil Producing Countries in the Belt and Road. *Resour. Sci.* **2017**, *39*, 1071–1083.

61. Sui, L.; Wang, J.; Yang, X.; Wang, Z. Spatial–Temporal Characteristics of Coastline Changes in Indonesia from 1990 to 2018. *Sustainability* **2020**, *12*, 3242. [[CrossRef](#)]
62. Monirul Qader Mirza, M. Global Warming and Changes in the Probability of Occurrence of Floods in Bangladesh and Implications. *Glob. Environ. Change* **2002**, *12*, 127–138. [[CrossRef](#)]
63. Mayaux, P.; Holmgren, P.; Achard, F.; Eva, H.; Stibig, H.-J.; Branthomme, A. Tropical Forest Cover Change in the 1990s and Options for Future Monitoring. *Philos. Trans. R. Soc. B Biol. Sci.* **2005**, *360*, 373–384. [[CrossRef](#)]
64. Giri, C.; Zhu, Z.; Tieszen, L.L.; Singh, A.; Gillette, S.; Kelmelis, J.A. Mangrove Forest Distributions and Dynamics (1975–2005) of the Tsunami-Affected Region of Asia. *J. Biogeogr.* **2008**, *35*, 519–528. [[CrossRef](#)]
65. Trung Thanh, H.; Tschakert, P.; Hipsey, M.R. Moving up or Going under? Differential Livelihood Trajectories in Coastal Communities in Vietnam. *World Dev.* **2021**, *138*, 105219. [[CrossRef](#)]
66. Mohamed-Chérif, F.; Ducruet, C. Regional Integration and Maritime Connectivity across the Maghreb Seaport System. *J. Transp. Geogr.* **2016**, *51*, 280–293. [[CrossRef](#)]
67. Rezaie, A.M.; Ferreira, C.M.; Rahman, M.R. Storm Surge and Sea Level Rise: Threat to the Coastal Areas of Bangladesh. In *Extreme Hydroclimatic Events and Multivariate Hazards in a Changing Environment*; Elsevier: Amsterdam, The Netherlands, 2019; pp. 317–342, ISBN 978-0-12-814899-0.

Disclaimer/Publisher’s Note: The statements, opinions and data contained in all publications are solely those of the individual author(s) and contributor(s) and not of MDPI and/or the editor(s). MDPI and/or the editor(s) disclaim responsibility for any injury to people or property resulting from any ideas, methods, instructions or products referred to in the content.